International Journal of Engineering, Mathematical and Physical Sciences
ISSN: 2517-9934
Vol:8, No:8, 2014

Mathematical Modeling of Cell Volume Alterations under Different Osmotic Conditions

Juliana A. Knocikova, Yann Bouret, Médéric Argentina, Laurent Counillon

***Abstract*—**Cell volume, together with membrane potential and intracellular hydrogen ion concentration, is an essential biophysical parameter for normal cellular activity. Cell volumes can be altered by osmotically active compounds and extracellular tonicity.

In this study, a simple mathematical model of osmotically induced cell swelling and shrinking is presented. Emphasis is given to water diffusion across the membrane. The mathematical description of the cellular behavior consists in a system of coupled ordinary differential equations. We compare experimental data of cell volume alterations driven by differences in osmotic pressure with mathematical simulations under hypotonic and hypertonic conditions. Implications for a future model are also discussed.

***Keywords*—**Eukaryotic cell, mathematical modeling, osmosis, volume alterations.

I. Introduction

CELLULAR volume has been shown to play an important role in the maintenance of intracellular osmolarity, cell shape, migration, cell proliferation, apoptosis, and regulation of intracellular metabolism [1], [2]. For example, it has been demonstrated that proliferation is stimulated by osmotic swelling or inhibited by osmotic shrinkage, respectively [3], [4]. On the other side, osmotic shrinkage is an early event in apoptosis [5], [6]. Under hypertonic conditions, the influx of extracellular osmotically active species compensates for a decreased cell volume, through the osmotically-coupled entry of water. Cells incapable of this regulatory volume increase are sensitive to apoptosis [7]. Apoptosis-related cell shrinkage is associated with the inhibition of sodium-hydrogen anti-porter 1 (NHE-1) [4].

The importance of regulatory pathways related to cell volume is crucial, even during pathophysiological conditions. For example, cell swelling is resulting from a decreased blood plasma osmolarity – hyponatremia, which occurs in situations where hormonal and renal function is impaired. This condition is accompanied by an increased intracellular osmolarity during cellular acidosis and hypoxia [8].

Cell volume alterations are caused by changes in intracellular osmolytes, secretion of electrolytes, Na^+ - dependent sugar / amino acid uptake, stimulation of Na/H exchange, Na-K-2Cl contraport with insulin and growth factors, to name a few. During osmotic adaptation, the ion concentration difference across the cell membrane causes solvent (water) transport and creates an osmotic pressure difference. Under anisotonic conditions, changes in cell volume are mostly based on cell membrane permeability to water, until equalization of the osmotic pressure difference. Thus, a new osmotic equilibrium of the water across the cell plasma membrane can be reached. Water diffusion transfer across the cell membrane is propagated through lipid bilayer and facilitated by protein channels, called aquaporins [9].

In this study, a simple model of cell swelling and shrinking by osmosis is introduced. The proposed approach aims to simulate the cell behavior in the case of continuously changing volume. Thus, mathematical descriptions of cellular behavior consist of coupled system of ordinary differential equations. Osmotic adaptation is measured by experimental data of cell volume alterations, driven by differences of osmotic pressure across the cell membrane. Mathematical simulations and experimental data were performed under different hypotonic and hypertonic conditions.

II. Methodology

A. Experimental Procedures

Cell volumes were acquired by spinning disk confocal microscopy, using 3-D image reconstruction of roughly 50 confocal planes for several different clusters of cells (with different number of cells, shapes and individual volumes in each cluster).

Changes in cell volume were observed under different extracellular osmolarities. The value of 300 mOsm, with a pH value of 7.4, was considered as isotonic. We performed experiments under different extracellular osmolarities for both hypotonic and hypertonic conditions. The initial hypotonic solution (<300 mOsm) was prepared as a mixture of 10 mMol/l KCl, 1mMol/l $CaCl_2$, 1mMol/l $MgCl_2$, 2 mMol/l glucose and 15 mMol/l HEPES in water. The hypertonic solution (> 300 mOsm) was prepared as a mixture with volumes of 1Mol/l Mannitol in water. Prepared solutions have been combined to reach the needed osmolarity. During experiments, hypertonic conditions were examined at an osmolarity of 350, 400, 450, 500 and 800 mOsm. Hypotonic conditions were established at 110, 150, 200 and 250 mOsm.

For each cell cluster, volumes were normalized according to initial values (Fig. 1). Hamster PS120 cells, a clone derived from CCL39 cells [10] that expresses no Na+/H+ exchanger, were used.

J. A. Knocikova is with Université de Nice – Sophia Antipolis, Institut Non Linéaire de Nice, CNRS-UMR 7335, Nice, France (e-mail: Juliana.Knocikova@unice.fr).

Y. Bouret is with Université de Nice – Sophia Antipolis, Laboratoire de Physique de la Matière Condensée, CNRS-UMR 7336, Nice, France

M. Argentina is with Université de Nice – Sophia Antipolis, Institut Non Linéaire de Nice, CNRS-UMR 7335, Nice and Institut Universitaire de France, Paris, France.

L. Counillon is with Université de Nice – Sophia Antipolis, Laboratoire de PhysioMédecine Moléculaire, CNRS-UMR 7370, Nice, France.

B. Mathematical Modeling

The mathematical description of cellular behavior consists of the coupled system of two ordinary differential equations, solved by numerical integration. The intracellular concentration and cell volume parameters were calculated using MATLAB.

To derive the first differential equation of the system, we considered the flux of water through the cell membrane. Differences in osmotic pressure over cell membrane were established to be the driving force. We proceeded from the changes of volumetric flow rate, which is described as an evolution of cell volume over time (1):

$$Q = \frac{dV}{dt}. \tag{1}$$

The second differential equation of the system describes the temporal evolution of the intracellular ion concentration during adaptation of the cell volume due to osmosis (2):

$$c_s(t) = \frac{n_s(t)}{V(t)}. \tag{2}$$

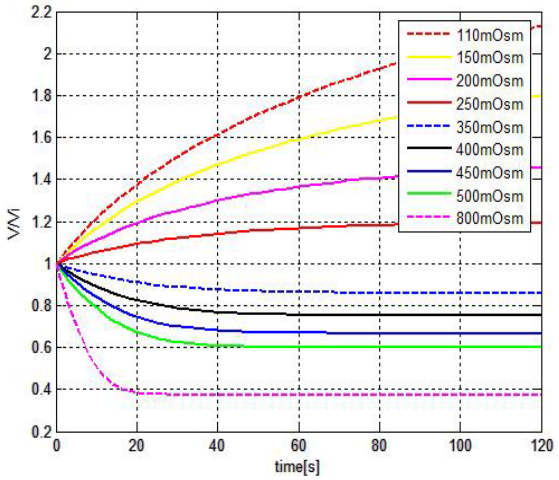

Fig. 1 Mathematical simulation of different osmotic conditions (represented by different osmotic pressures) of the extracellular space. Value of cell volume is normalized to its starting point V_i.

III. Results

Solvent Flux (Water) – 1. Equation of the System:

As stated before, the volumetric flow rate Q is defined using (1).

Moreover, the volumetric flow rate is proportional to the water flow, j, the surface area, S, and the water density, ρ (3):

$$Q = \frac{j.S}{\rho}. \tag{3}$$

Next, the solvent (water) flux j is defined as

$$j = \lambda(\Delta P - \Delta \Pi), \tag{4}$$

where λ is a coefficient of the membrane permeability for water, $\Delta P = P_F - P_P$ is a hydraulic pressure difference between feed and permeate side of the membrane and $\Delta\Pi = \Pi_F - \Pi_P$ is an osmotic pressure difference. In our model, we neglected ΔP and the $\Delta\Pi$ was established as the only driving force.

The osmotic kinetics are governed by the difference in the solvent chemical potential across the cell membrane. According to the van't Hoff's law, we considered the osmotic pressure to be directly proportional to the solution concentration (5), where R is the universal gas constant and T is the absolute temperature:

$$\Pi = RTc. \tag{5}$$

Finally, using (1), (3), (5), we derived the first differential equation of the system:

$$\frac{dV}{dt} = \frac{\lambda(-RT(c_S - c_{out}))S}{\rho}. \tag{6}$$

Ions Flow – 2. Equation of the System:

Using intracellular concentration (2) and changes in the amount of constituent (in moles of substance being dissolved)

$$dn_s = -j_s S(t)dt, \tag{7}$$

we computed the first order expansion of the intracellular concentration:

$$c_s(t+dt) = \frac{n_s(t) + dn_s}{V(t+dt)} = c_s(t) + dc_s, \tag{8}$$

which allowed us to derive

$$c_s(t+dt) = c_s(t) - j_s \frac{S}{V} dt - c_s(t) \frac{dV}{V}. \tag{9}$$

Accordingly, changes in intracellular concentration over time due to the osmotic adaptation, could be formulated as:

$$\frac{dc_s}{dt} = -\frac{c_s}{V}\frac{dV}{dt} - j_s \frac{S}{V}. \tag{10}$$

Using the described approach, we get a coupled system of ordinary differential equations as:

$$\begin{cases} \dfrac{dV}{dt} = \dfrac{\lambda(-RT(c_S - c_{out}))S}{\rho} \\ \dfrac{dc_s}{dt} = -\dfrac{c_s}{V}\dfrac{dV}{dt} - j_s \dfrac{S}{V}. \end{cases} \tag{11}$$

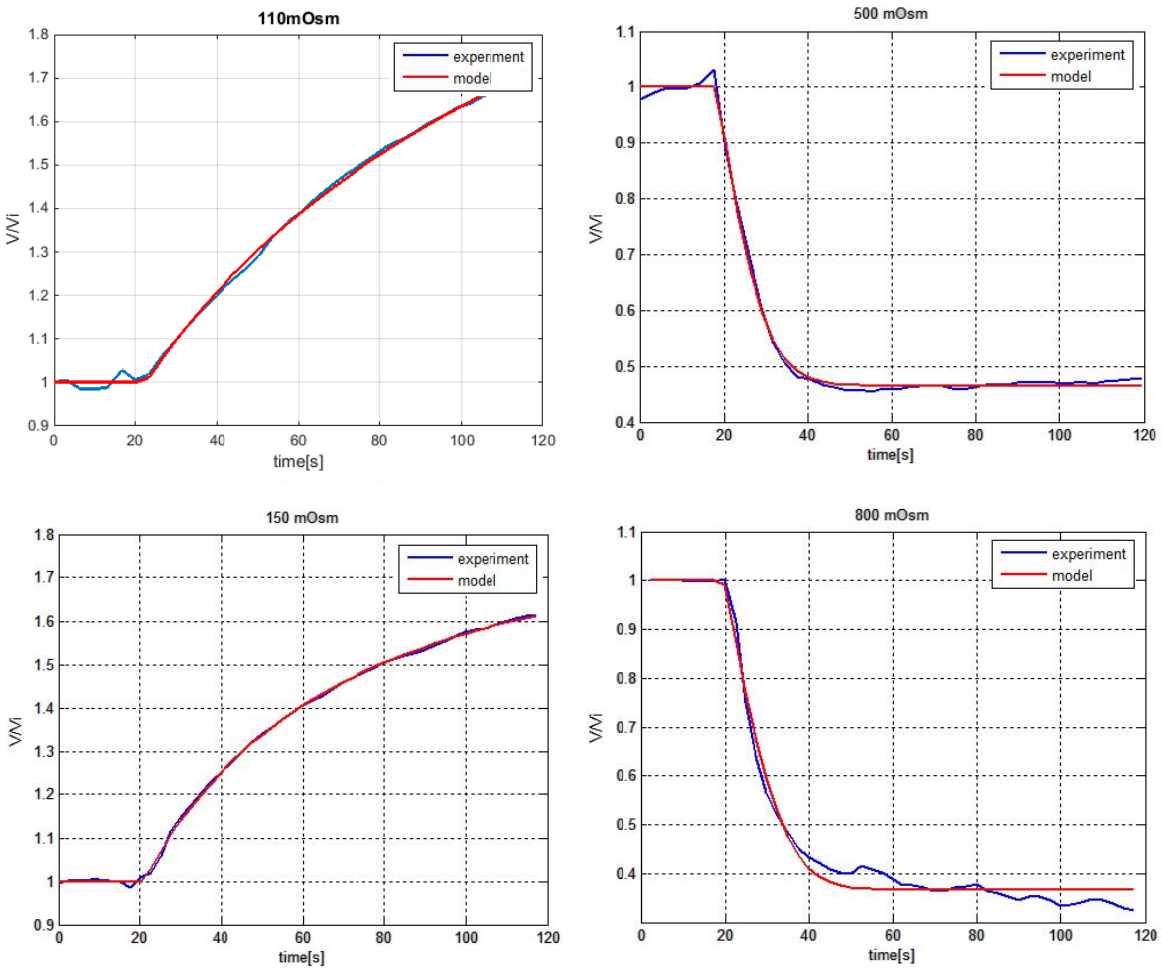

Fig. 2 Examples of experimental values (blue line) fitted with model equations (red line) for different hypotonic (110 mOsm, 150 mOsm) and hypertonic (500mOsm, 800 mOsm) conditions. Cell volume is normalized to the initial value V_i

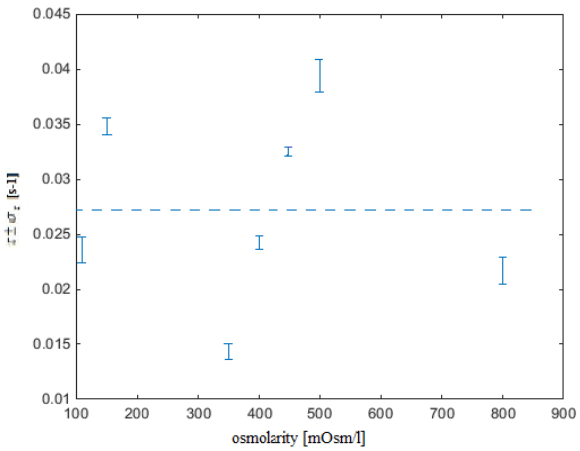

Fig. 3 Error bars of time constants calculated from fitting the experimental volume data with model curves, expressed as a function of external osmolarity Dashed line: average value (0.0272±0.0087)s^{-1}

Because the concentration changes are directly proportional to the osmotic pressure difference, this model is working with the proportion between hyper/hypotonic and isotonic values. Thus, volume alterations due osmotic adaptation have been mathematically simulated for different osmolarities (Fig. 1). Measured cell volumes were fitted with model curves of volume alterations (Fig. 2).

According to the proposed system of differential equations (11), we derived a model theoretical time constant as follows

$$\tau = \frac{\lambda RTc_0 S_0}{\rho V_0}. \quad (12)$$

Equation (3) is indeed derived from the Fick's law for water flow through cell membrane of thickness l with diffusion coefficient Dc. Permeability P of cell membrane for water is thus expressed as a proportion between diffusion coefficient and the membrane thickness in units of speed:

$$P = \frac{Dc}{l}. \quad (13)$$

Thus, we finally get a theoretical time constant as a function of water velocity through cell membrane (15):

$$\tau = \frac{\lambda RTc_0 S_0}{\rho V_0} = \frac{Dc}{l}\frac{M_W RTc_0 S_0}{RT\rho V_0} \quad (14)$$

$$\tau = \frac{Dc}{l}\frac{M_W c_0 S_0}{\rho V_0} \quad (15)$$

Subsequently, corresponding time constants resulting from fitting experimental volume data with model curves have been assessed for each given osmolarity. We did not observe statistically significant variances between established time constants as a function of changing osmolarity (Fig. 3).

Using (14), we derived formula for water permeability

$$\frac{Dc}{l} = \frac{\tau\rho V_0}{M_W c_0 S_0}. \quad (16)$$

Thus, for each given osmolarity, we were able to calculate corresponding permeability of water. The following example shows a calculation for a hypotonic condition of 110 mOsm/l, and a corresponding time constant τ=0,023 s^{-1}.

$$\frac{Dc}{l} = \frac{0{,}023 s^{-1}.997 kg.m^{-8}.7{,}74.10^{-15} m^3}{0{,}018 kg.mol^{-1} 0{,}3 Mol.m^{-3}.1{,}9.10^{-9} m^2} = 0{,}0168 m.s^{-1} \quad (17)$$

Values of water permeability for given set of examined osmolarities were falling within interval between 0,016 – 0,028 $m.s^{-1}$.

IV. Discussion

The main purpose of this paper was to build a simplified mathematical model of cell volume alterations, that enable to test different osmotic experimental conditions. The emphasis has been given to water diffusion through the cell membrane. We followed a classical approach based on Fick's and van't Hoff 's laws of cell osmotic adaptation. This leads to a simple computational method for derivation the water permeability through cell membrane.

Water propagates through animal cell membrane mainly via lipid bilayer and water-selective protein channels, aquaporins. Values of water permeability through cell lipid bilayer has been observed to be very low (P=0,0022 $cm.s^{-1}$, [12]; P=0,0042 $cm.s^{-1}$, [13]). Such observations are in accordance with a widely accepted solubility – diffusion theory related to transport of small molecules across lipid bilayers.

On the other side, aquaporins significantly increase the osmotic water permeability. High values of water permeabilities are typical especially for kidney proximal convoluted tubule (P=500.$10^{-3}$$cm.s^{-1}$) [14], containing mainly AQP1 and APQ7. To determinate the contribution of AQP1 to water permeability of nephrons, water permeability has been compared between wild-type (P=0,26 ± 0,02 $cm.s^{-1}$) and AQP1 knockout mice (P=0,031 ± 0,007 $cm.s^{-1}$) [15]. Similarly, high water permeability has been observed also for an epithelial cells in the cochlear apex co-expressing AQP4 and AQP5 (P=156,9.10^{-3} $cm.s^{-1}$) [16]. High permeability of water is in accordance with a low Arhenius activation energy for water transport through membranes that contain aquaporins (E_r = 4-6 kcal/mol), under comparison with activation energy of water movement across a lipid membrane (E_r = 8-10 kcal/mol). Such a low activation energy is similar to the activation energy for self-diffusion of water or for the viscous transport of water [17].

It has been suggested that the value of water permeability P<0,005 $cm.s^{-1}$ is reflecting a diffusion purely through lipid portion of the membrane. P>0,01 $cm.s^{-1}$ suggests the involvement of water channels in transport [18]. This concept is today widely used in determinating the presence of aquaporin activity. According to those criteria, a very high contribution of aquaporin activity on water permeability during osmotic adaptation of PS120 cells is suggested.

However, our model of cell volume alterations is built with few significant simplifications. At first, mechanical pressure and the surface tension have not been taken into account and the osmotic pressure difference has been established as the only driving force during cell volume alterations.

The model primarily takes into account water diffusion across the cell membrane due to the osmotic adaptability. In that case, the cell membrane is impermeable to all the surrounding solute molecules and behaves as an ideal semipermeable membrane. Cell swelling or shrinking is exclusively based on adjustment of the tonicity of cell interior according to the changes in water concentration of extracellular space. Thus, we neglected the regulatory mechanisms of ion fluxes and expected the sum of them across cell membrane to reach zero at the beginning of osmotic adaptation. Therefore, we considered them to be zero in our equations, since they are not operating significantly at the time scales we are working. Under such conditions, we derived values of osmotic water permeability at the very beginning of cell osmotic adaptation for different osmolarities.

Osmotic water permeabilities differ significantly between different cell types. The ease of water penetration depends on the cell type and species of animal. Moreover, the current knowledge on mechanisms related to the volume regulation is revealing a great diversity related to the transport systems and signaling pathways. Cell volume thus remains a complex matter with significant physiological and pathophysiological consequences.

V. Conclusions

This paper is based on simplified mathematical model of the cell volume alterations with emphasis given to water diffusion across the membrane, driven by differences between intracellular and extracellular osmotic pressure. This leads to a simple computational method for derivation the water permeability through cell membrane.

Recent findings showed the importance of ion channel activity and related ion fluxes, as well as oxygen species in modulation of the cell volume patterns. Thus, our next

approach will include mechanisms of ion flow into the current model.

MODEL NOMENCLATURE

Variable

$\Delta\Pi$ osmotic pressure difference between intracellular and extracellular space – the driving force

Parameters

c_S molar concentration within cell
c_{out} molar concentration outside cell
D_C diffusion coefficient
j solvent (water) flux
j_S flux of the particles (ions)
l cell membrane thickness
n amount of constituent, moles of substance being dissolved
P cell membrane permeability for water
ΔP pressure difference across the membrane (hydraulic) – between feed side and permeate side of the membrane
Q volumetric flow rate
R universal gas constant
S surface membrane area
T thermodynamic temperature
V cell volume
λ coefficient of water permeability
ρ density of water

Used Constants and Figures:

M_W molecular weight of water (0.018 kg.mol^{-1})
ρ density of water (997 kg.m^{-3} at 25 °C)
c_0 molar concentration corresponding to isotonic conditions (300 mOsm.l^{-1})
S_0 surface membrane area of hamster fibroplast [11] (1,9.10^{-9} m^2)
V_0 corresponding volume under isotonic conditions (7,74.10^{-15} m^3)

ACKNOWLEDGEMENT

The authors declare no conflict of interest. This study has been supported by the University of Nice-Sophia Antipolis, the CNRS Bio Maths Info PEPS 2012 and the INSERM "Physique-Cancer" Program (H+ Cancer).

REFERENCES

[1] G.I. Evan, K.H. Vousden, "Proliferation, cell cycle and apoptosis in cancer," in *Nature*, vol. 411, pp. 342-348, 2001.
[2] F.Q. Alenzi, "Links between apoptosis, proliferation and the cell cycle," in *Br J Biomed Sci*, vol. 61, pp. 99-102, 2004.
[3] R.S. Wong, "Apoptosis in cancer: from pathogenesis to treatment," in *J Exp Clin Cancer Res*, 30:87, 2011.
[4] D.L. Grossmann, L. Huc, X. Terkli, "A role of NHE-1 in cell proliferation and migration," in *Cell Apoptotic Signaling Pathways*, (ed. Ch.O. Pickens), *Nova Science Publishers*, pp. 86-109, 2007.
[5] Y. Okada, E. Maeno, "Apoptosis, cell volume regulation and volume-regulatory chloride channels," in *Comp Biochem Physiol A Mol Integr Physiol*, vol. 130, pp. 377–383, 2001.
[6] M.B. Friis, C.R. Friborg, L. Schneider, "Cell shrinkage as a signal to apoptosis in NIH 3T3 fibroblasts, " in *J Physiol, vol.* 567, pp. 427–443, 2005.
[7] C.D. Bortner, J.A. Cidlowski, „Cell shrinkage and monovalent cation fluxes: role in apoptosis" in *Arch Biochem Biophys*, vol. 462, pp. 176-188, 2007.
[8] B. Nilius, J. Eggermont, T. Voets, G. Buyse, V. Manolopoulos, G. Droogmans, "Properties of volume-regulated anion channels in mammalian cells," in *Prog Biophys Mol Biol*, vol. 68, pp. 69–119, 1997.
[9] A. S. Werkman, "Aquaporins at glance," in *J of Cell Sci*, vol 124, pp. 2107- 2112, 2011.
[10] J. Pouyssegur, C. Sardet, A. Franchi, G. Allemain, A. Paris, "A specific mutation abolishing Na+/H+ antiport activity in hamster fibroblasts precludes growth at neutral and acidic pH," in *Proc Natl Acad Sci USA*, vol. 81, pp. 4833– 4837, 1984.
[11] On-line database: http://bionumbers.hms.harvard.edu/bionumber.aspx?&id=105877&ver=2#
[12] A. Finkelstein, "Water and nonelectrolyte permeability of lipid bilayer membranes," in *J Gen Physiol*, vol. 68, pp.127-135, 1976.
[13] K. Olbrich, W. Rawicz, D. Needham, F. Evans," Water permeability and mechanical strength in polyunsaturated lipid bilayers," in *Biophys J*, vol. 79, pp. 321-327, 2000.
[14] C.A. Berry, A.S. Verkman, "Osmotic gradient dependence of osmotic water permeability in rabbit proximal convoluted tubule, " in *J Membr Biol*, vol. 105, pp. 33-43, 1988.
[15] C.L. Chou, M.A. Knepper, A.N. VanHeok, D. Brown, T. Ma, A.S. Verkman, "Reduced water permeability and altered ultrascructure in thin descending limb of Henle in aquaporin-1 null mice," in *J Clin Invest*, vol. 103, pp. 491-496, 1999.
[16] A. Eckhart, M. Müller, A. Salt, J. Smolders, H. Rask-Andersen, H. Löwenheim, "Water permeability of mammalian cochlea: functional features of an aquaporin-facilitated water shunt at the perilymphendolymph barrier," in *Eur J Physiol*, vol. 466, pp. 1963-1985, 2014.
[17] R.I. Macey, "Transport of water and urea in red blood cells, " in *Am J Physiol*, vol. 246, pp. C195-C203, 1984.
[18] A.S Werkman, A.N. VanHoek, T. Ma, A. Frigeri, W.R. Skach, A. Mitra, B.K. Tamarappoo, J. Farinas, "Water transport across mammalian cell membranes," in *Am J Physiol*, vol. 270, pp. C12-C30, 1996.